



## Prediction and optimization of fuel cell performance using a multi-objective genetic algorithm

Gustavo Marques Hobold<sup>1</sup>, Ramesh K. Agarwal<sup>2</sup>

<sup>1</sup> Laboratory of Energy Conversion Engineering & Technology, Federal University of Santa Catarina, Florianópolis, Brazil & Washington University in St. Louis, MO 63130, USA.

<sup>2</sup> Department of Mechanical Engineering & Materials Science, Washington University in St. Louis, MO 63130, USA.

### Abstract

The attention that is currently being given to the emission of pollutant gases in the atmosphere has made the fuel cell (FC), an energy conversion device that cleanly converts chemical energy into electrical energy, a good alternative to other technologies that still use carbon-based fuels. The temperature plays an important role on the efficiency of an FC as it influences directly the humidity of the membrane, the reversible thermodynamic potential and the partial pressure of water; therefore the thermal control of the fuel cell is the focus of this paper. We present models for both high and low temperature fuel cells based on the solid-oxide fuel cell (SOFC) and the polymer electrolyte membrane fuel cell (PEMFC). A thermodynamic analysis is performed on the cells and the methods of controlling their temperature are discussed. The cell parameters are optimized for both high and low temperatures using a Java-based multi-objective genetic algorithm, which makes use of the logic of the biological theory of evolution to classify individual parameters based on a fitness function in order to maximize the power of the fuel cell. Applications to high and low temperature fuel cells are discussed.

*Copyright © 2013 International Energy and Environment Foundation - All rights reserved*

**Keywords:** Fuel cell; SOFC; PEMFC; Genetic algorithm; Thermal control; Thermodynamic efficiency; Optimization.

### 1. Introduction

Because of the clean and high density energy they provide and their potential applications, fuel cells have drawn a lot of attention in the last few decades. Two types of fuel cells have received the greatest attention; they are the Proton Exchange Membrane and the Solid Oxide Fuel Cells (PEMFC and SOFC, respectively), both operate under different temperature ranges. While the PEMFC works in a temperature range from 300 to 400°C [1], the SOFC may operate at much higher temperatures, sometimes even close to 1100°C [2]. Much has been done in fuel cell modeling and experimentation [1-15], but those models are not always optimized for best performance. In this paper, we present models for both low and high temperature fuel cells and optimize their parameters. We also analyze the influence of each design parameter in the performance of the fuel cell.

The construction and operation of a high temperature fuel cell is many times restricted by external factors and for these reasons the low temperature fuel cells, especially the PEMFC, have been more explored and researched. The restriction factors on high temperature fuel cells include issues related to

good water management and/or the manufacturing of a membrane that operates under acceptable power output even without proper humidification [16]. The humidification is a huge problem because in high temperature fuel cells such as the SOFC, the water output from the chemical reaction is in the vapor phase due to the high temperature. In order to maintain water in its liquid state, impracticable pressures are necessary, as can be seen from Figure 1. Another reason for the manufacturing of a high temperature fuel cell is difficult is because the membrane is often made of ceramic which goes through a thermal expansion in a confined space; since ceramic is a brittle material, it causes it to crack unexpectedly. On the other hand, high temperature fuel cells offer a higher power output than the low temperature fuel cells and the heat lost in its operation may be used for other purposes, such as operating a steam turbine for cogeneration [7, 13]. Because of problems with the mechanical resistance due to high temperature of fuel cells, they are mostly limited to stationary applications [9].

The goal of this paper is to employ a multi-objective genetic algorithm in order to optimize the parameters of both a high temperature and low temperature fuel cell. We create a family of points that would produce a desirable outcome, for example maximizing the power as well as minimizing the pressure exerted on both the cathode and the anode. As design parameters, we use the temperature, the current density, the pressure exerted on the cathode and anode, as well as the mass fraction of each component (oxygen, hydrogen and water). We also analyze the effect of several design parameters.

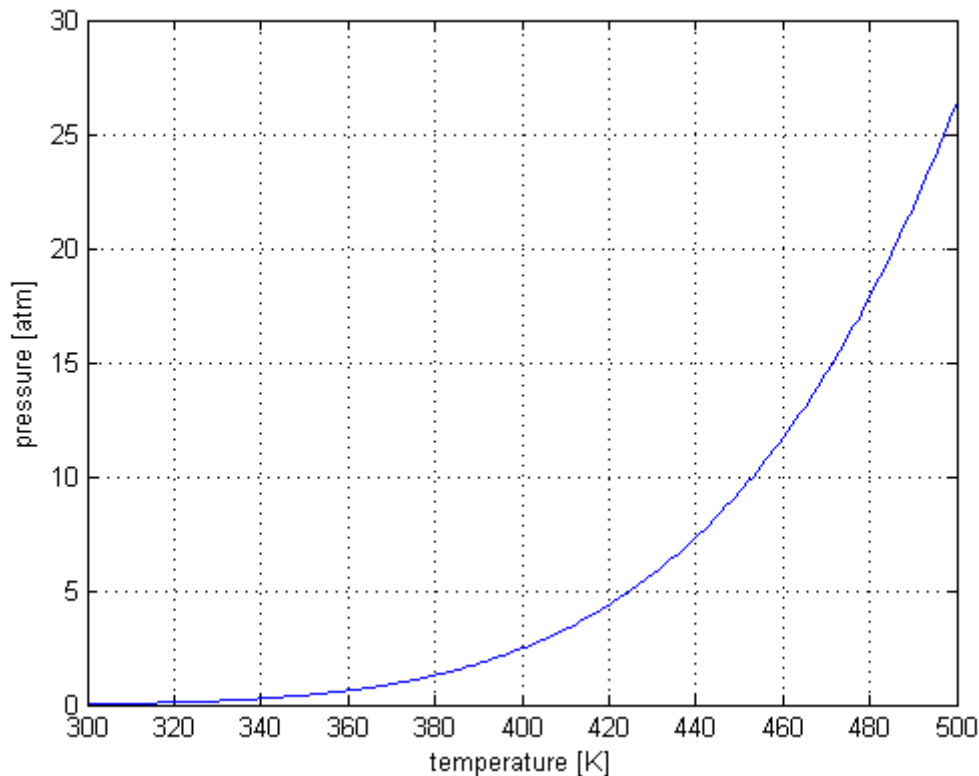


Figure 1. Saturation pressure of water as a function of temperature

As a first simulation tool, we use MATLAB to predict the performance of the fuel cell and then we employ the Java-based multi-objective genetic algorithm package jMetal [17], in which we run a modified version of the Kursawe problem [18], which allows us to choose any number of objectives, parameters and constraints, to optimize the performance of the fuel cell.

Because of the lower temperature operation, much has been done in the field of PEM fuel cells. The dynamics of the fuel cell has been discussed in [19] and the control modeling for automotive use has been discussed in [11], in these papers the authors discuss a transient model, including the study of mass flow and inertia dynamics as well as the manifold filling dynamics. Fuel cell stack systems have been discussed in [14], where a stack of 125 PEMFC is used for model validation.

As for SOFC, many of the models include different geometry. We can find models for planar cells [7, 8], cylindrical cells [13], and tubular cells [2]. There are also studies in anode and cathode supported fuel cells [7] and their effects on the performance [6].

One of the main concerns of fuel cells operations is water management. Even though there is some work done in this area [16], the subject is still under a great deal of research and requires attention, especially since it is known that humidity and water management play a major role in fuel cell performance [20].

## 2. Fuel cell models

Fuel cells are devices that convert chemical energy into electrical energy. Because of the complex modeling requirements, Computational Fluid Dynamics (CFD) has been a major player in full scale comprehensive simulations. In this paper, we focus our efforts to the optimization of a simpler fuel cell model that does not require complex CFD simulations. Obtaining a good model is a difficult task, mainly because it is necessary to capture the complex phenomena such as multi-species gas mixtures and fluid flow, heat transfer, electrochemical reactions, and diffusion through the layers.

For both SOFC and PEMFC, we assume a planar model with 3 main layers: (1) the anode, (2) the electrolyte, and (3) the cathode as shown in Figure 2.

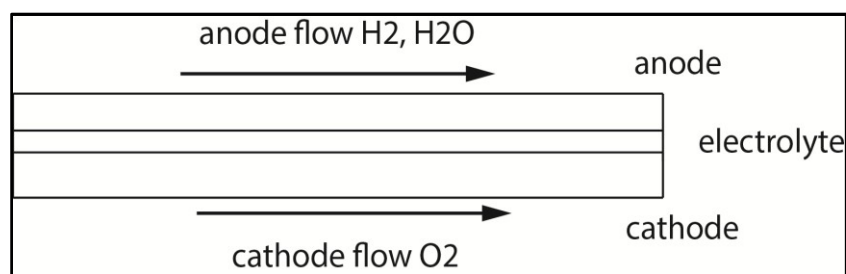


Figure 2. Structure of the fuel cell

The main reaction is the same for both types of fuel cells: the oxidation of the hydrogen and thus the formation of water. The oxygen flows in the cathode and is adsorbed at the cathode and thus is reduced by electrons coming from the external load:



The hydrogen is then adsorbed in the anode and the oxygen ion reacts with the hydrogen:



The overall reaction is then given by:



### 2.1 Analysis of the reversible fuel cell

Just like any other thermodynamic system, a fuel cell can be analyzed as a reversible heat engine. The good thing about this approximation is that the FC may be considered as a black box control volume, for which one does not need to know the underlying physical phenomena or how to model them. One can then proceed by considering that the system simply has an input of oxygen and hydrogen at a certain temperature and pressure, and gives outputs of work, heat and water also at a certain temperature and pressure. Figure 3 presents the reversible fuel cell modeled as a black box control volume, with the inflow of oxygen and hydrogen, and outflow of water, work and heat.

As discussed in [21], the fuel cell efficiency is given by:

$$e = \frac{w}{-\Delta h(T)} = \frac{\Delta g(T)}{\Delta h(T)} \quad (4)$$

The reversible efficiency as a function of temperature is shown in Figure 4.

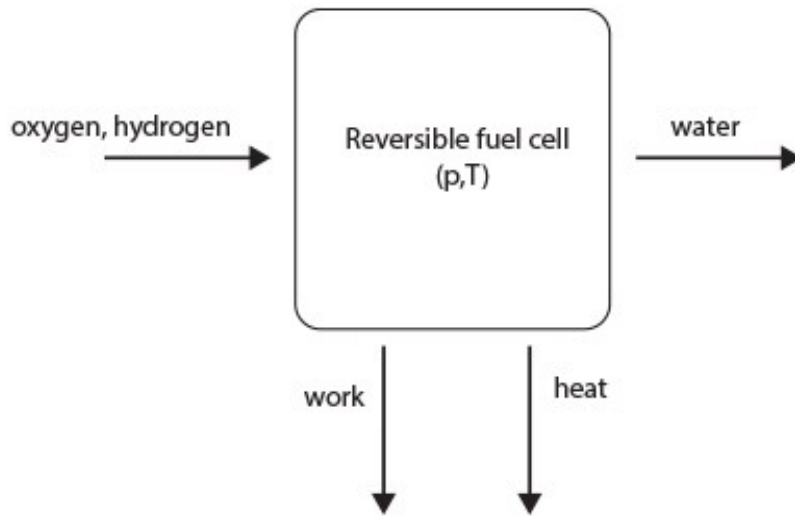


Figure 3. Outline of the reversible fuel cell

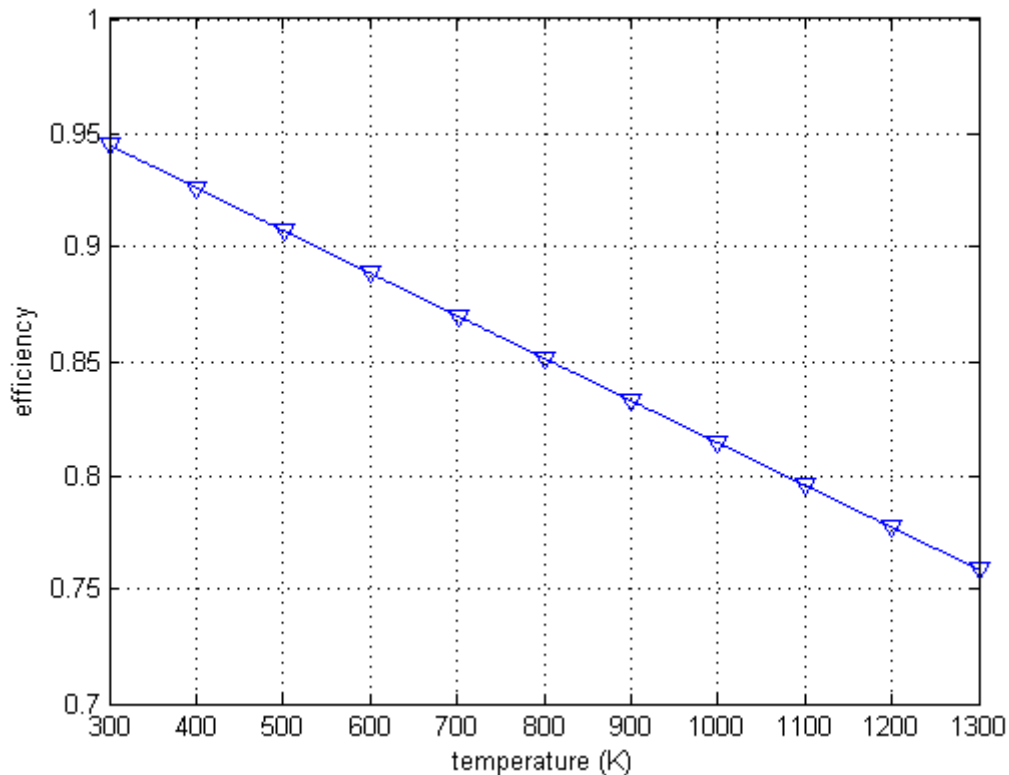


Figure 4. Reversible fuel cell efficiency as a function of temperature

### 2.2 Solid oxide fuel cell model

The SOFC model is used as a baseline for the prediction of a high temperature fuel cell. The model presented here includes the influence of the theoretical thermodynamic voltage as well as activation, concentration and ohmic losses. The output voltage is then given by:

$$V = E - \eta_{act,an} - \eta_{act,ca} - \eta_{ohm,el} - \eta_{ohm,ca} - \eta_{ohm,an} - \eta_{con,an} - \eta_{con,ca} \quad (5)$$

where  $\eta_{act}$  are the activation losses for the cathode and the anode;  $\eta_{ohm}$  are the ohmic losses for the electrolyte, the cathode and the anode;  $\eta_{con}$  are the concentration losses for the cathode and the anode; and  $E$  is the thermodynamic potential given by the Nernst equation.

### 2.2.1 Thermodynamic potential

The thermodynamic potential may be expressed by the Nernst equation [6]:

$$E = E^0(T) + \frac{RT}{nF} \ln \left( \frac{p_{cathode}^{0.5} x_{O_2}^{0.5} x_{H_2}}{x_{H_2O}} \right) \quad (6)$$

where  $R = 8.3145 \frac{J}{mol \cdot K}$  is the universal gas constant,  $F = 96485 \frac{C}{mol}$  is the Faraday constant,  $n = 2$  is the number of reactant electrons,  $p_{cathode}$  is the cathode pressure,  $x$  is the mass fraction of each component and  $E^0(T)$  is the reversible potential, expressed by:

$$E^0(T) = -\frac{\Delta G(T)}{nF} \quad (7)$$

and  $\Delta G(T)$  is the variation in the Gibbs free energy given by:

$$\Delta G(T) = \Delta H(T) - T \left( \Delta S^0 + \int_{T_{ref}}^T \frac{\Delta C_p(T)}{T} dT \right) \quad (8)$$

$$\Delta H(T) = \Delta H^0 + \int_{T_{ref}}^T \Delta C_p(T) dT \quad (9)$$

$$\Delta C_p = C_{p,H_2O} - C_{p,H_2} - 0.5C_{p,O_2} \quad (10)$$

The heat capacity is interpolated by a polynomial (Table 1) [22]:

$$C_p(T) = \sum_{i=0}^6 a_i T^i \quad (11)$$

Table 1. Heat capacity coefficients

	$a_0$	$a_1$	$a_2$	$a_3$	$a_4$	$a_5$	$a_6$
$H_2O$	37.373	-41.205	146.05	-217.08	181.54	-79.409	14.015
$O_2$	34.85	-57.975	203.68	-300.37	231.72	-91.821	14.776
$H_2$	21.157	56.036	-150.55	199.29	-136.15	46.903	-6.4725

It is also important to note that the mass fraction of the water is dependent on the mass fraction of the hydrogen in such a way that

$$x_{H_2O} = 1 - x_{H_2} \quad (12)$$

as they are both present in the cathode only. Furthermore, it can be seen that the thermodynamic potential is almost linearly dependent on the temperature.

### 2.2.2 Activation over-potential

The activation over-potential is the main loss in low current densities even though it increases with the current, its derivative is much stronger when  $i$  is small.

Because the reaction is not always initiated as fast as intended by the thermodynamic analysis, there are losses associated with the number of reactions taking place in the fuel cell. It is important to note that increasing the rate at which the chemical reaction takes place can increase the output of the system. The activation over-potential is the loss associated with the delay of the reactants that actually enter the

cathode/anode and react with the electrolyte. This delay is sometimes said to be an energy barrier which the reaction has to overcome before full power [2]. For this reason, there are activation losses associated with both the cathode and the anode. We use the Butler-Volmer equation to express the activation over-potential.

$$i = i_{o,a} \left[ \exp\left(\alpha_a \frac{nF}{RT} \eta_{act,a}\right) - \exp\left(-\alpha_c \frac{nF}{RT} \eta_{act,a}\right) \right] \quad (13)$$

$$i = i_{o,c} \left[ \exp\left(\alpha_a \frac{nF}{RT} \eta_{act,c}\right) - \exp\left(-\alpha_c \frac{nF}{RT} \eta_{act,c}\right) \right] \quad (14)$$

These equations need to be solved for the activation over-potential and are solved by an iterative method. We choose Newton's method with a maximum error of  $1e5$ . The parameters used in the equations are  $\alpha_a, \alpha_c, i_o$ , which are the charge transfer coefficients for the anode and cathode and the exchange current density respectively. The exchange current density is obtained from an equation described in [7]:

$$i_{o,a} = \gamma_a \left(\frac{p_{H_2}}{p_{ref}}\right) \left(\frac{p_{H_2O}}{p_{ref}}\right) \exp\left(-\frac{E_{act,a}}{RT}\right) \quad (15)$$

$$i_{o,c} = \gamma_c \left(\frac{p_{O_2}}{p_{ref}}\right)^{0.25} \exp\left(-\frac{E_{act,c}}{RT}\right) \quad (16)$$

### 2.2.3 Ohmic over-potential

The ohmic, also called resistant, over-potential is due to the impossibility of a smooth charge transport through the membrane of the fuel cell. Furthermore, as electrons and ions must be transported, the resistance associated with both parts must be taken into account. The modeling of this phenomenon requires the specification of a membrane. We take in consideration the resistivity of the electrolyte, the cathode and the anode, although most of the time the contribution of the last two may be neglected.

As the electrolyte of a SOFC is ceramic, its conductivity at low temperature is very low and increases quickly as higher temperatures are achieved. This profile is provided in [7]:

$$\sigma_e = \rho_e^{-1} = \beta_1 \exp\left(-\frac{\beta_2}{T}\right) \quad (17)$$

The conductivity of both anode and cathode are considered constant in the temperature range studied in this paper. The ohmic losses are given by:

$$\eta_{ohm,e} = t_e \rho_e i \quad (18)$$

$$\eta_{ohm,a} = t_a \rho_a i \quad (19)$$

$$\eta_{ohm,c} = t_c \rho_c i \quad (20)$$

where  $\rho$  is the resistivity and  $t$  is the thickness of each component.

### 2.2.4 Concentration over-potential

The concentration overvoltage is due to the mass transport across the cell. If the ions and electrons manage to pass through the membrane, they may face a "crowding" on the other side because the outputs of the cell may not be optimized and thus the flow will not be uniform, causing the particles to stack in the exit and thus causing a huge loss of energy, especially at high current densities. In high temperature fuel cells, the concentration losses are often neglected, as they are considered not to be of great influence and furthermore their modeling can be very complicated. In low temperature fuel cells, however, they have a huge role in limiting the current. Ref. [7] describes a reliable model for this kind of loss.

$$\eta_{conc,c} = -\frac{RT}{2nF} \ln\left(\frac{1}{x_{O_2}} - \left(\frac{1}{x_{O_2}} - 1\right) \exp\left(\frac{RT t_c}{2eF D_{eff,c} p_{cat\ hode}}\right)\right) \quad (21)$$

$$\eta_{conc,a} = -\frac{RT}{2nF} \ln \left( \frac{1 + \frac{iRT t_a}{nF D_{eff,a} p_{H_2}}}{1 + \frac{iRT t_a}{nF D_{eff,a} p_{H_2O}}} \right) \quad (22)$$

where  $D_{eff}$  is the effective diffusion coefficient.

### 2.2.5 Parameters and properties

The parameters and properties used in running the model are shown in Table 2. These parameters are taken from [6-8, 13]. We take  $p_{cathode}$ ,  $p_{anode}$ ,  $T$ ,  $i$ ,  $x_{O_2}$ ,  $x_{H_2}$  as design parameters for our optimization. The thermodynamic potential and the losses described are plotted in Figures 5 and 6 for  $x_{O_2} = x_{H_2} = 0.97$  and  $p_{cathode} = p_{anode} = 3 \times 10^5 Pa$ .

Table 2. Parameters for the SOFC

Parameter	Value
$\gamma_a$	$5.5 \times 10^8 A/m^2$
$\gamma_c$	$7 \times 10^8 A/m^2$
$E_{act,a}$	$140 \times 10^3 J/mol$
$E_{act,c}$	$137 \times 10^3 J/mol$
$\alpha_a$	0.5
$\alpha_c$	0.3
$\beta_1$	$20500 \Omega^{-1} m^{-1}$
$\beta_2$	9030 K
$\rho_a$	$3.3 \times 10^{-5} \Omega m$
$\rho_c$	$7.7 \times 10^{-5} \Omega m$
$t_a$	0.1 mm
$t_c$	1 mm
$t_e$	0.1 mm
$D_{eff,a}$	$2.1 \times 10^{-5} m^2/s$
$D_{eff,c}$	$5.4 \times 10^{-6} m^2/s$
$H^0$ (HHV)	$-242 \times 10^3 J/mol$
$S^0$	$-44.4 J/mol-K$
$p_{ref}$	101.33 kPa

### 2.3 Proton exchange membrane fuel cell

The PEMFC is used as a model to simulate a low temperature fuel cell. The model we describe here is much simpler than the one used to simulate the high temperature fuel cell, but still is widely used in the literature. We include the thermodynamic potential as well as ohmic, activation and concentration losses, without distinction from the electrolyte, cathode or anode.

$$V = E - \eta_{act} - \eta_{ohm} - \eta_{con} \quad (23)$$

#### 2.3.1 Thermodynamic potential

The thermodynamic potential (Nernst equation) can also be written for low temperatures and small temperature variations as:

$$E = E_o + \frac{\Delta S}{2F} (T - T_{ref}) + \frac{RT}{2F} \ln \left( \frac{p_{H_2} \sqrt{p_{O_2}}}{p_{H_2O}} \right) \quad (24)$$

At standard temperatures and pressures (STP), this equation reduces to [15]:

$$E = 1,229 - 8.5 \times 10^{-4} (T - 298) + 4.308 \times 10^{-5} T \ln \left( \frac{p_{H_2} \sqrt{p_{O_2}}}{p_{H_2O}} \right) \quad (25)$$

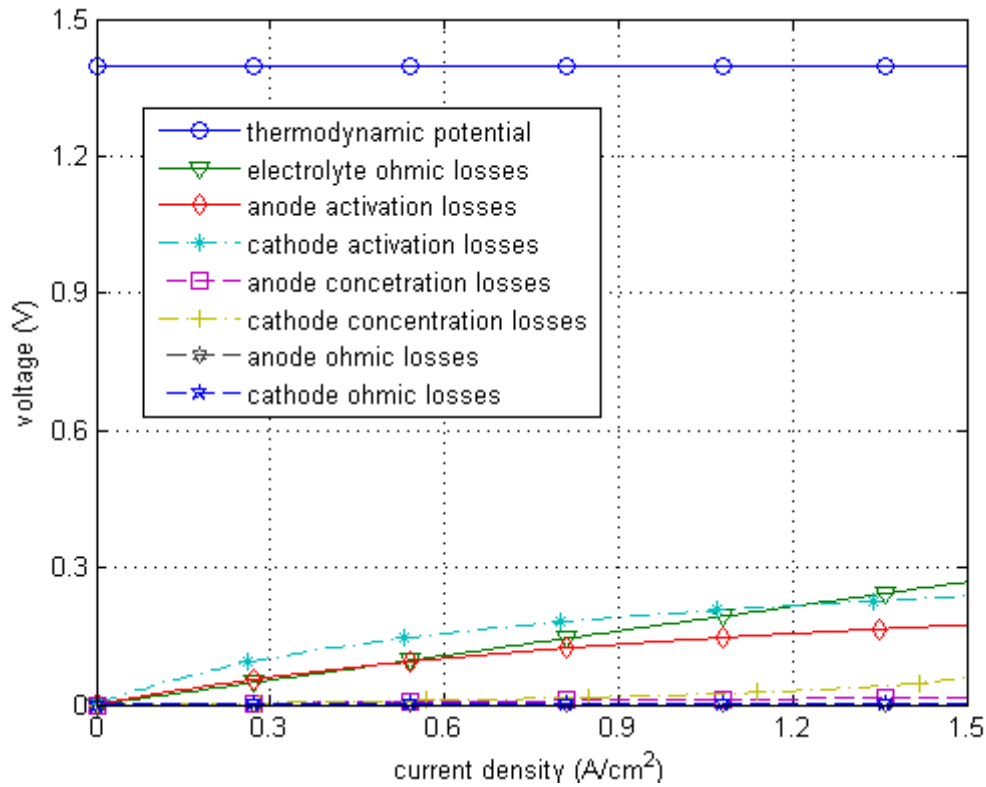


Figure 5. Potentials as a function of current density for  $T = 1100\text{K}$

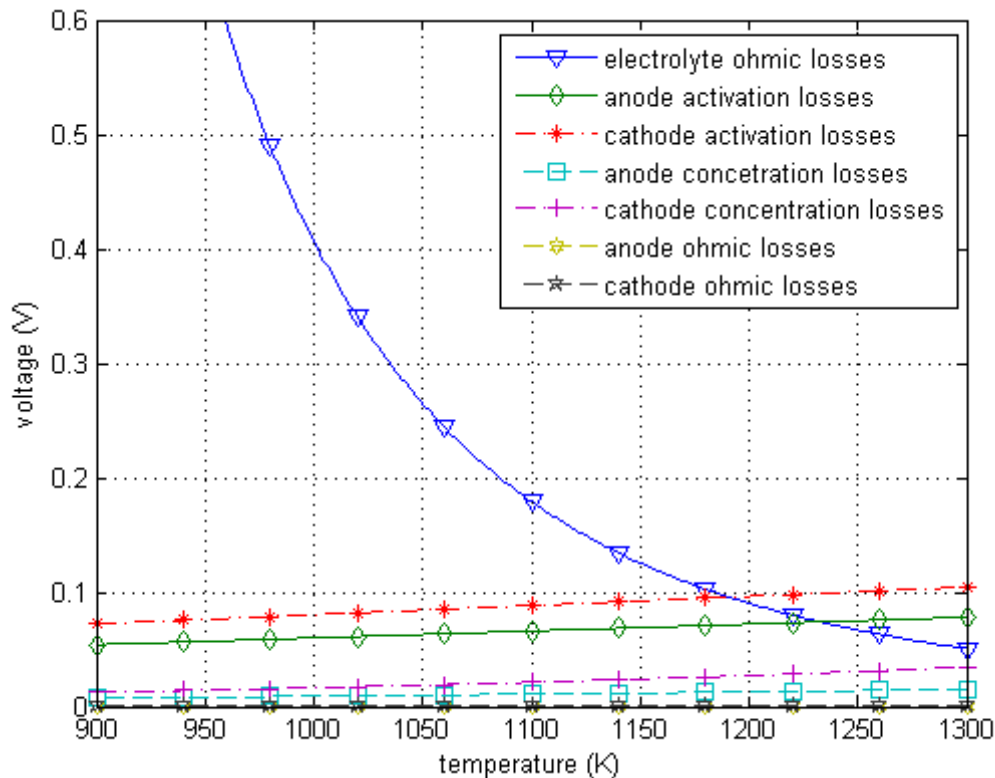


Figure 6. Potentials as a function of temperature for  $i = 1 \text{ A/cm}^2$

### 2.3.2 Activation over-potential

The model we adopt for the activation over-potential was validated by Pukrushpan et al. [11] for an automotive fuel cell; it can be used for any PEMFC system as long as the membrane is well humidified (which we expect to be) and the pressures are controlled. It can be written as:

$$V_{act} = V_o + V_a(1 - e^{-c_1 i}) \quad (26)$$

$$V_o = 0.279 - 8.5 \times 10^{-4}(T - 298) + 4.3085 \times 10^{-5}T \left\{ \ln \left( \frac{p_{cat\ hode} - p_s}{1.101325} \right) + \frac{1}{2} \ln \left[ \frac{0.1173(p_{cat\ hode} - p_s)}{1.01325} \right] \right\} \quad (27)$$

$$V_a = (-1.618 \times 10^{-5}T + 1.618 \times 10^{-2}) \left( \frac{p_{O_2}}{0.1173} + p_s \right)^2 + (1.8 \times 10^{-4}T - 0.166) \left( \frac{p_{O_2}}{0.1173} + p_s \right) - 5.8 \times 10^{-4}T + 0.5736 \quad (28)$$

where  $p_s$  is the saturation pressure of water at a given temperature. In some investigations, the saturation pressure of water is held constant during the optimization or the method used to track it is not described [15]. However, the saturation pressure of water is strongly dependent on temperature, and thus in this paper we suggest the use of Wagner's equation [23].

$$\ln \left( \frac{p_s}{p_c} \right) = (a_1 t + a_2 t^{1.5} + a_3 t^3 + a_4 t^{3.5} + a_5 t^4 + a_6 t^{7.5}) \frac{T_c}{T} \quad (29)$$

where  $p_c$  and  $T_c$  are the critical pressure and temperature of the desired substance and  $t = 1 - T/T_c$ . For water, the coefficients of the equation are shown in Table 3. The plot is shown in Figure 1.

Table 3. Coefficients of Wagner's equation

$a_1$	$a_2$	$a_3$	$a_4$
-7.8595173	1.8448259	-11.7866497	22.6807411
$a_5$	$a_6$	$p_c$	$T_c$
-15.9618719	1.80122502	220.64 atm	647.096 K

### 2.3.3 Ohmic over-potential

The membrane used in this study is the Nafion-117. The model presented accounts for both the resistance of the ionic and electronic transport [24].

$$V_{ohm} = i(r_{el} + r_{ion}) \quad (30)$$

$$r_{el} = \frac{t_m}{\sigma} \quad (31)$$

$$r_{ion} = t_m \left\{ \frac{181.6 \left[ 1 + 0.03i + 0.062 \left( \frac{T}{303} \right)^2 i^{2.5} \right]}{(\lambda_m - 0.634 - 3i) \exp \left[ 4.18 \left( \frac{T-303}{T} \right) \right]} \right\} \quad (32)$$

$$\sigma = \frac{1}{b_{11}\lambda_m - b_{12}} \exp \left[ b_2 \left( \frac{1}{T} - \frac{1}{303} \right) \right] \quad (33)$$

where  $r$  are the ionic and electronic resistances,  $t_m$  is the membrane thickness [cm],  $\sigma$  is the membrane conductivity [ $\Omega^{-1}\text{cm}^{-1}$ ],  $\lambda_m$  is the membrane humidification factor which varies from 14 (dry) to 24 (highly supersaturated). Figure 7 highlights the importance of membrane humidification.

### 2.3.4 Concentration over-potential

For the concentration overpotential, we use a very general model described in [25]:

$$V_{con} = -\frac{RT}{2F} \left( 1 + \frac{1}{\alpha} \right) \ln \left( 1 - \frac{i}{i_{max}} \right) \quad (34)$$

As mentioned before when describing the SOFC, for high temperature fuel cell the concentration over-potential does not play a major role. In low temperature fuel cell however, it often limits the maximum current admitted. In Figure 8, this effect is illustrated by setting  $i_{max} = 1 \text{ A/cm}^2$ . The charge transfer coefficient usually varies between 0.3 and 0.5.

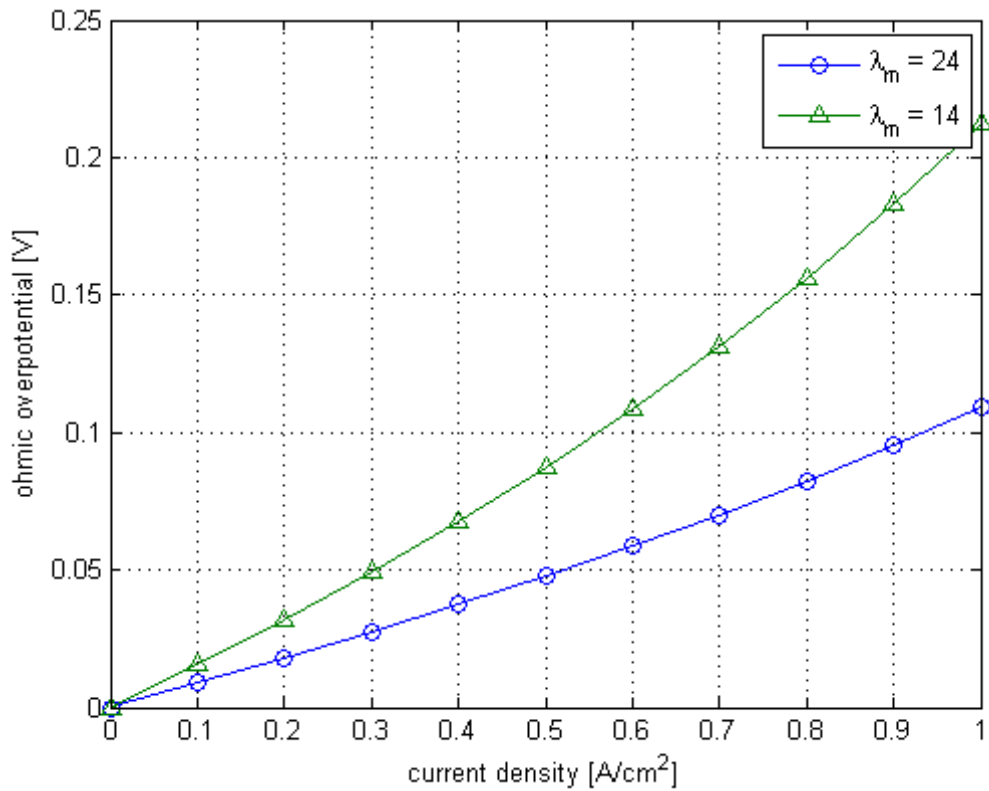


Figure 7. Influence of membrane humidification in the ohmic over-potential

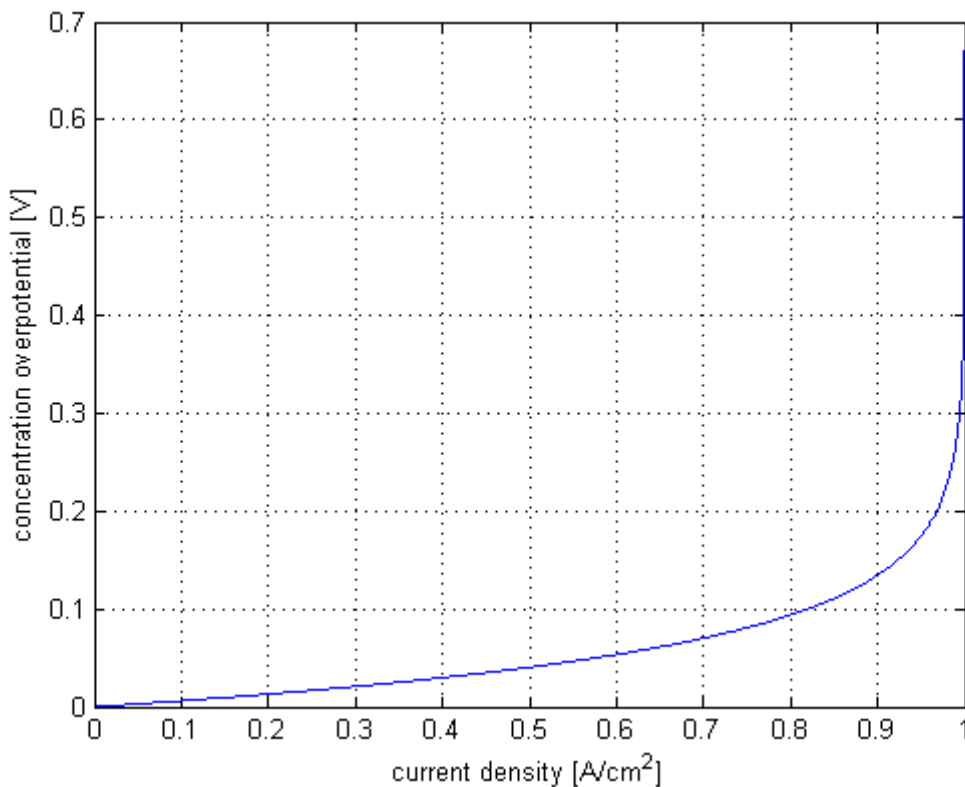


Figure 8. Influence of the limiting current in the concentration over-potential

### 3. Brief description of the genetic algorithm

In this section, we briefly describe the genetic algorithm (GA) and discuss the techniques it uses to obtain the optimized result.

### 3.1 Single objective genetic algorithms (SOGA)

Genetic algorithms are a class of stochastic optimization algorithms inspired by the biological evolution. In GA, a set or *generation* of input vectors, called *individuals*, is iterated over, successively combining traits (aspects) of the best individuals until a convergence is achieved. In general, GA employs the following steps [26].

1. **Initialization:** Randomly create N individuals.
2. **Evaluation:** Evaluate the fitness of each individual.
3. **Natural selection:** Remove a subset of the individuals. Often the individuals that have the lowest fitness are removed; although culling, the removing of those individuals with similar fitness, is sometimes performed.
4. **Reproduction:** Pick pairs of individuals to produce an offspring. This is often done by roulette wheel sampling; that is, the probability of selecting some individual  $h_i$  for reproduction is given by:

$$P[h_i] = \frac{\text{fitness}(h_i)}{\sum_j \text{fitness}(h_j)} \quad (35)$$

A *crossover* function is then performed to produce the offspring. Generally, crossover is implemented by choosing a crossover point on each individual and swapping *alleles* or vector elements at this point as illustrated in Figure 9.

5. **Mutation:** Randomly alter some small percentage of the population.
6. **Check for Convergence:** If the solution has converged, return the best individual observed. If the solution has not yet converged, label the new generation as the current generation and go to step 2. Convergence is often defined by a certain number of generations or a similar threshold.

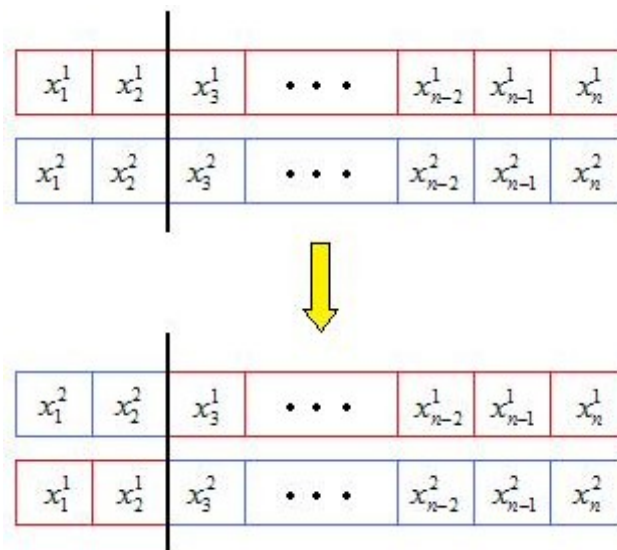


Figure 9. Illustration of the general crossover function in genetic algorithm (GA)

### 3.2 Multi-objective genetic algorithm (MOGA)

For many design problems, it is desirable to achieve, if possible, simultaneous optimization of multiple objectives [27]. These objectives, however, are usually conflicting, preventing simultaneous optimization of each objective [28]. Therefore, instead of searching for a single optimal solution, a multi-objective genetic algorithm is necessary to find a set of optimal solutions (generally known as Pareto-optimal solutions). For Pareto-optimal solutions, any individual inside the set dominates any individual outside the set while any individual in the set is not dominated by another individual in this solution set. The MOGA algorithms used to find the Pareto-optimal solutions to the airfoil optimization problem in this study is widely known as NSGA-II [29]. It has the following three features: (1) it uses an elitist principle, (2) it uses an explicit diversity preserving mechanism, and (3) it emphasizes non-dominated solutions in a population. The implementation procedure of NSGA-II is as follows [17]:

1. **At 0-th generation**, a random parent population  $P_0$  of size  $N$  is created; it is sorted based on the non-domination. Then the individuals in  $P_0$  are ranked: 1 is the best level, 2 is the next-best level, and so on. Then  $P_0$  is sent to selection, recombination, and mutation operators to create offspring population  $Q_0$  of size  $N$ .
2. **At  $t$ -th generation**, a combined population  $R_t = P_t \cup Q_t$  of size  $2N$  is formed and is sorted according to non-domination. Then individuals in  $R_t$  are divided into the best non-dominated set  $F_1$ , the next-best non-dominated set  $F_2$  and so on. If the size of  $F_1$  is smaller than  $N$ , all members of  $F_1$  go to  $P_{t+1}$ , with the remaining members chosen from  $F_2, F_3 \dots$  until the size of  $P_{t+1}$  is  $N$ . Then new population  $P_{t+1}$  are sent to selection, crossover, and mutation operators to create a new population  $Q_{t+1}$  of size  $N$ .
3. **Termination**: the procedure terminates when convergence criterion is met.

### 3.3 Fuel cell optimization

In the study of the solid oxide high temperature fuel cell, we conduct two kinds of studies: we perform a single-objective optimization to maximize the output power, leaving the temperature, the cathode and anode pressures and the mass fraction of the hydrogen and oxygen as optimization parameters. We then perform a multi-objective optimization to maximize the power and minimize the pressures on the cathode and anode, from which we obtain a Pareto-front set of solutions.

In the case of the low temperature fuel cell, we use only the single-objective optimization algorithm in order to maximize the power.

The boundaries of each optimization variable are described in Tables 4 and 5. We define a new function called  $i_{\max}(T)$  for the high temperature fuel cell. This function yields the non-trivial value of the current density for which the power density is zero. It is an analogy for the maximum current density which defines the concentration over-potential of the low temperature fuel cell.

Table 4. SOFC optimization parameters

Variable	Lower bound	Upper bound
Temperature [K]	900	1300
Cathode pressure [Pa]	$10^5$	$3 \times 10^5$
Anode pressure [Pa]	$10^5$	$3 \times 10^5$
O <sub>2</sub> mass fraction [ - ]	0.1	1
H <sub>2</sub> mass fraction [ - ]	0.1	1
Current density [A/cm <sup>2</sup> ]	0	$i_{\max}(T)$

Table 5. PEMFC optimization parameters

Variable	Lower bound	Upper bound
Temperature [K]	300	370
Oxygen pressure [atm]	0.21	3
Hydrogen pressure [atm]	1	3
Current density [A/cm <sup>2</sup> ]	0	$i_{\max}$
Humidifying coefficient	14	24
Cathode pressure [atm]	1	3

## 5. Results and discussion

The fuel cell models were coded in MATLAB for prior analysis and then implemented in a Java-based multi-objective genetic algorithm which was used for optimization, using the Kursawe problem [18] as a reference.

### 5.1 Optimization of the high temperature fuel cell

It is important to first analyze the behavior of the fuel cell model prior to optimization. Figure 10 shows the behavior of the solid oxide fuel cells for anode and cathode pressures of  $3 \times 10^5$  Pa and mass fractions of oxygen and hydrogen of 0.97. From this simulation, it is clear that a pattern emerges from which we can guess that the optimum temperature will be 1300K.

From Figure 11, it is also possible to see the influence of each kind of loss in the output voltage. The activation over-potential quickly drags the potential down for lower temperatures, while for higher temperatures it is possible to see some linearity and thus the influence of the ohmic loss. In none of them, however, the concentration over-potential is significant.

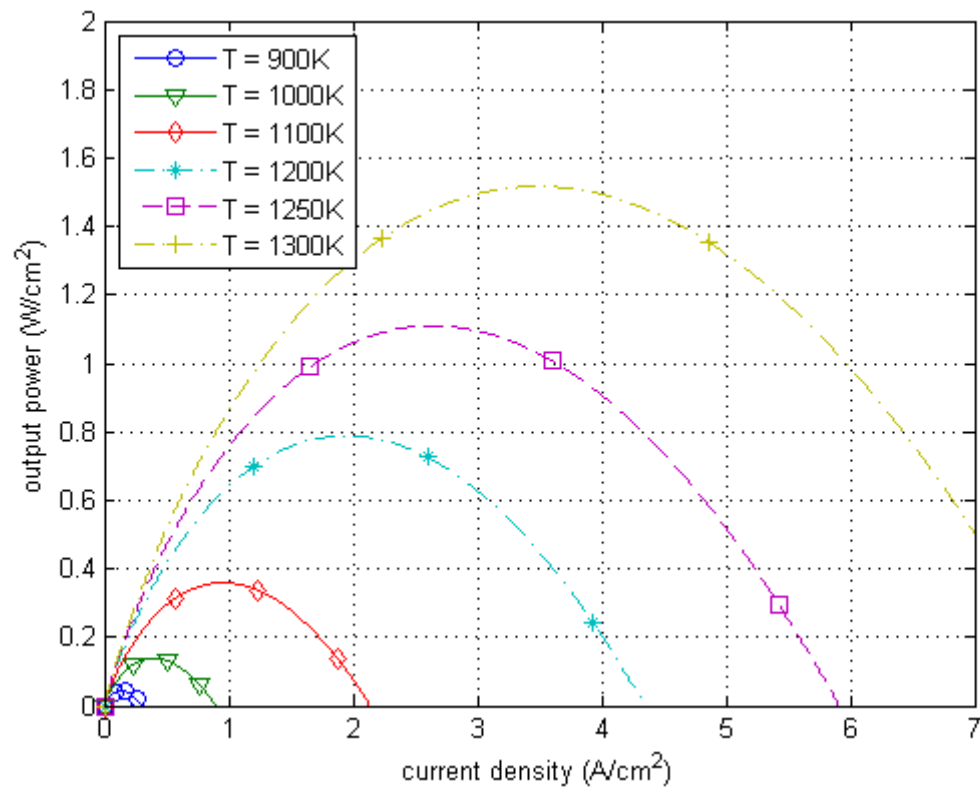


Figure 10. Power density as a function of current density for given temperatures

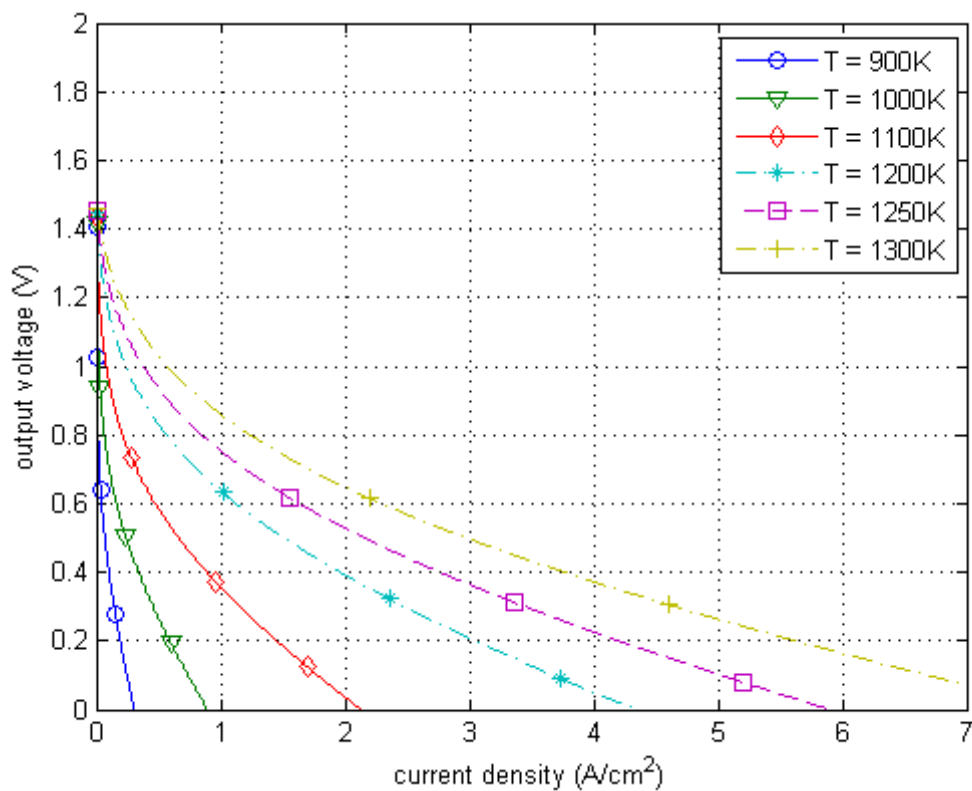


Figure 11. Output voltage as a function of the current density for given temperatures

We proceed with the optimization. First, we perform a single-objective optimization to simply maximize the power. The optimized value of each design variable is shown in Table 6. The optimum temperature, as expected, is the upper bound 1300K and so are the cathode and anode pressures and the O<sub>2</sub> mass fraction. The boundary of the H<sub>2</sub> mass fraction, however, is not active and thus it assumes a value different from the upper bound. This result confirms the need of research in better water management systems for fuel cells, because the H<sub>2</sub>O mass fraction fights with the H<sub>2</sub> mass fraction for the optimum value.

Next, we obtain a set of solution for some given values of temperature and thus optimize them for the maximum power. The boundaries of the cathode and anode pressures and of the temperature remain active, but the hydrogen mass fraction as well as the current density optimum value change. Figures 12, 13 and 14 show this analysis. It is interesting to note however that the model predicts the optimum power to grow very fast at very high temperatures, but manufacturing of fuel cells that resist such temperature without cracking and with sufficiently good water management is still very vague. Figure 13 shows the same pattern for current density. The importance of water management also appears again in Figure 14, which shows that in order to maintain maximum performance, the water fraction needed also increases with temperature (because  $x_{H_2O} = 1 - x_{H_2}$ ).

Table 6. SOFC optimum values

Variable	Optimum
Temperature [K]	1300
Cathode pressure [Pa]	$3 \times 10^5$
Anode pressure [Pa]	$3 \times 10^5$
O <sub>2</sub> mass fraction [ - ]	1
H <sub>2</sub> mass fraction [ - ]	0.733789
Current density [A/cm <sup>2</sup> ]	4.3088
Power [W/cm <sup>2</sup> ]	1.94855

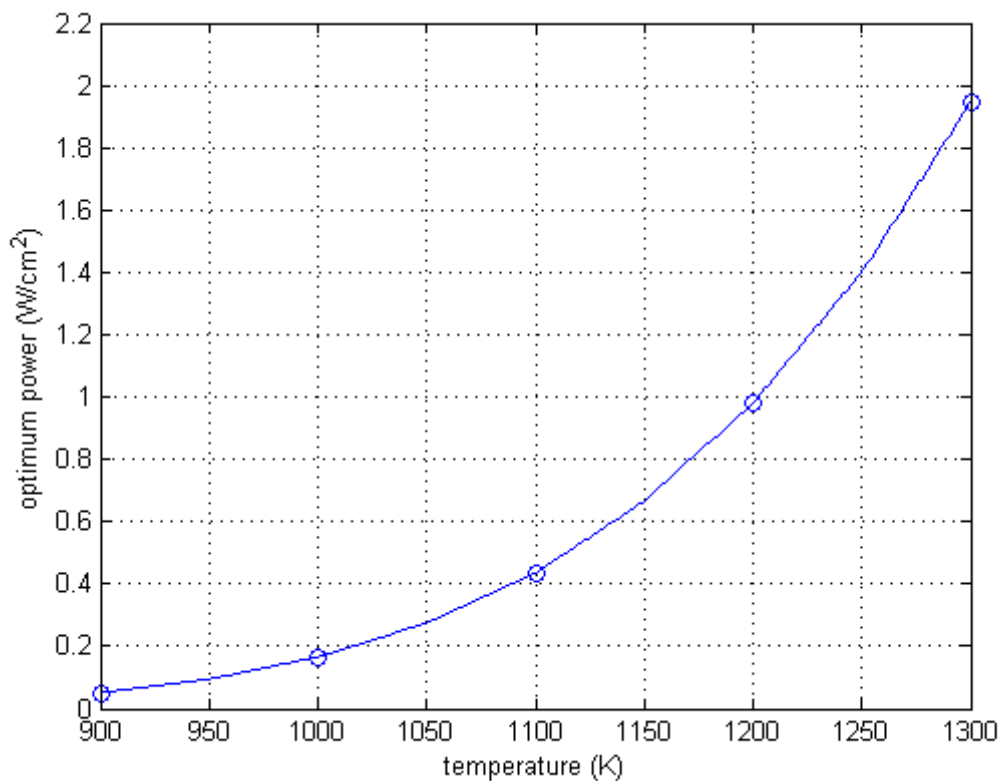


Figure 12. Optimum power density as a function of temperature

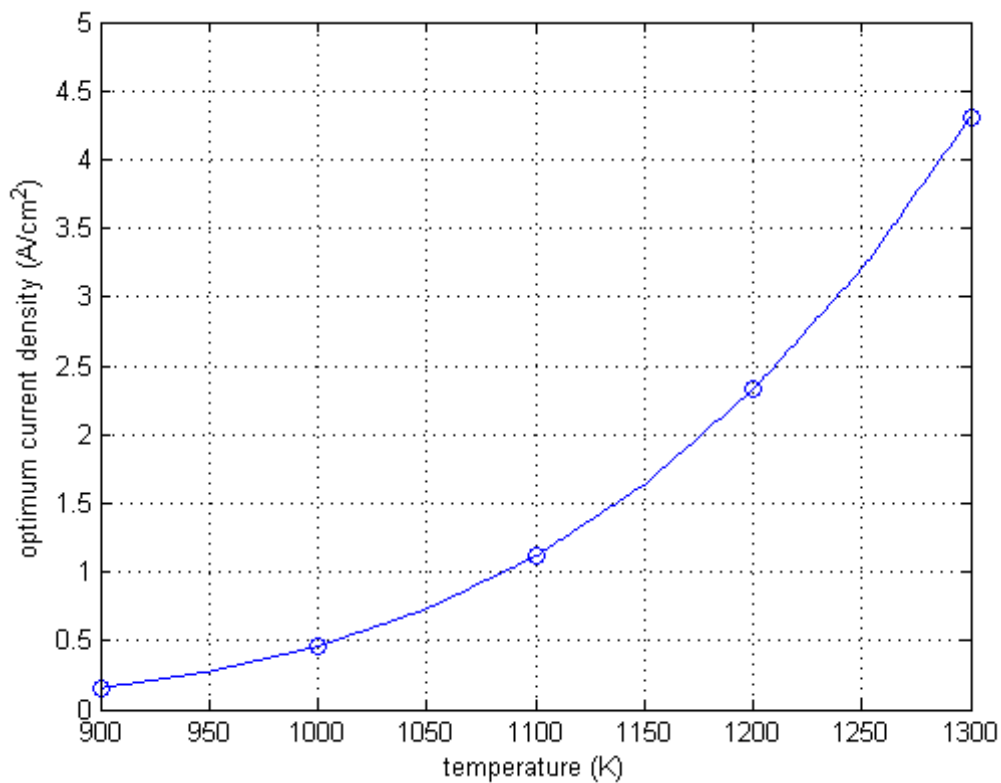


Figure 13. Optimum current density as a function of temperature

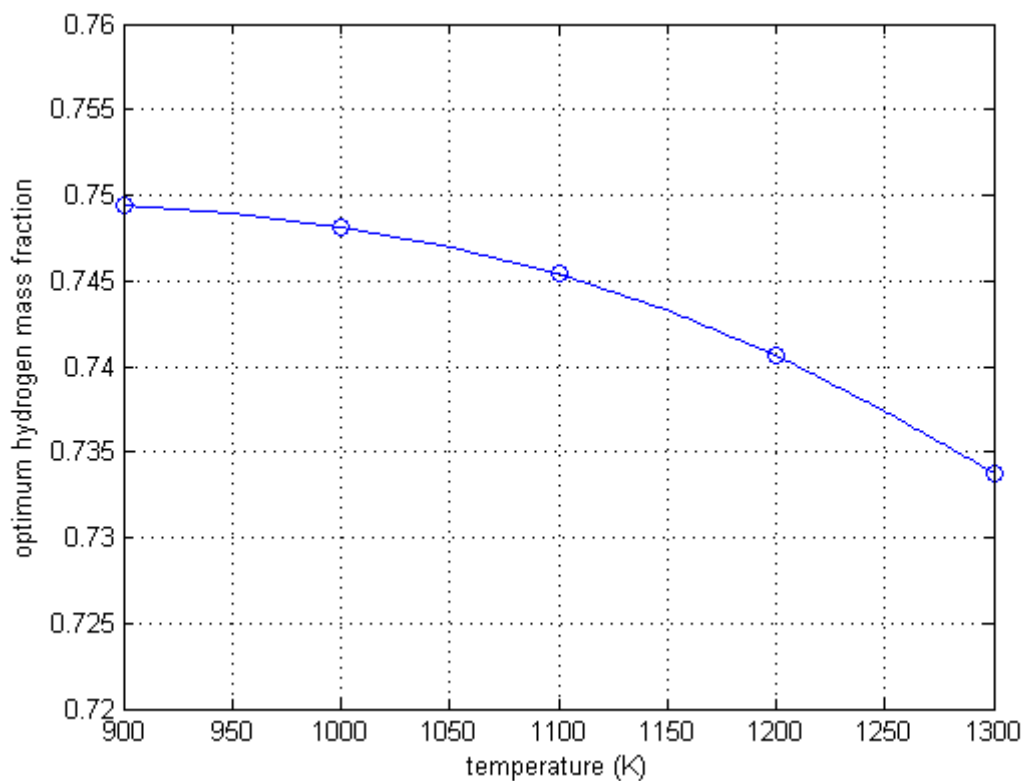


Figure 14. Optimum hydrogen mass fraction as a function of temperature

We now proceed to the multi-objective optimization in order to not only maximize power, but also to minimize the cathode and anode pressure. Even though the maximum power is obtained nonetheless when the cathode and anode pressures assume their upper bound value, the algorithm produces a Pareto-

front set of solutions which are plotted over the maximum power solution in Figure 15. This set of solutions provide many good points for an excellent performance while maintaining the pressures sufficiently low. For example, the Pareto-front has a solution for which both the pressures of cathode and anode are atmospheric. In this solution, the temperature and oxygen mass fraction remain boundary-active, they assume the values of the upper bound, the hydrogen mass fraction is 0.7247 and the power output is 0.8769 W/cm at a current density of 3.019 A/cm<sup>2</sup>.

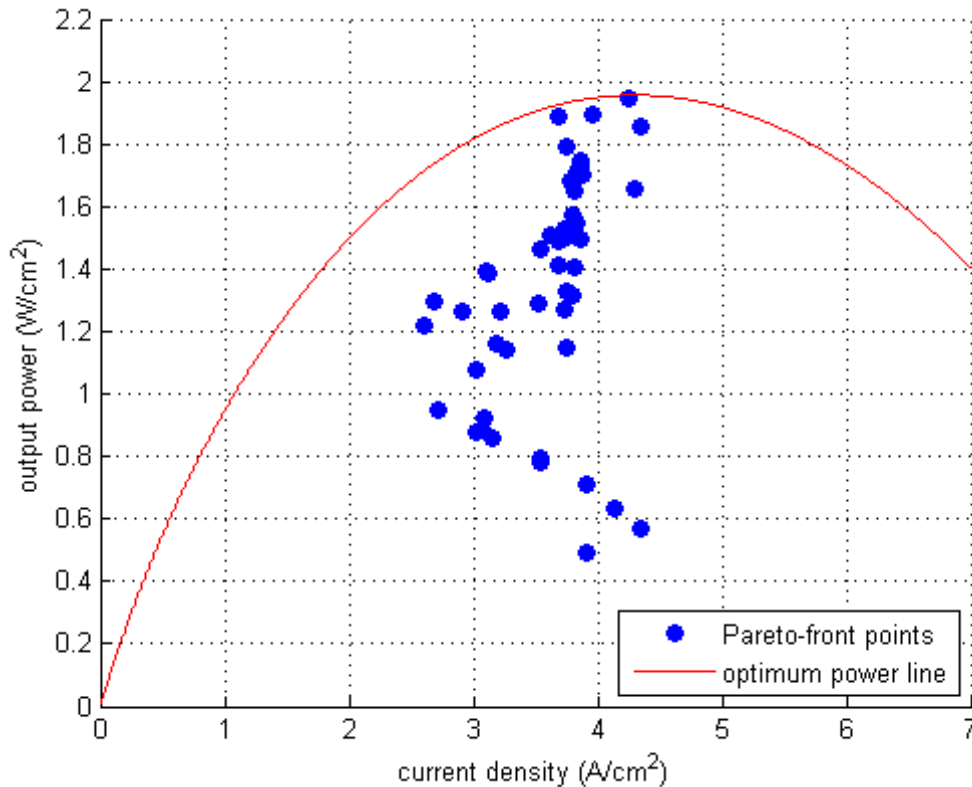


Figure 15. Plot of Pareto-front solutions

From the solution shown in Figures 12 and 13, we can determine the efficiency of the fuel cell when operating at its optimum condition and compare with the reversible efficiency in Figure 4.

We first determine the rate of hydrogen atom transfer  $z$  and then use it to determine the efficiency:

$$z = \frac{i}{nF} \quad (36)$$

Thus the efficiency is given by:

$$e_{real} = \frac{P}{-z\Delta h} \quad (37)$$

As shown in Figure 16, even though the reversible efficiency of the fuel cell decreases with temperature, the efficiency of the real fuel cell increases and is much smaller than the reversible one.

### 5.2 Optimization of the low temperature fuel cell

Similar to what was done with the high temperature fuel cell, we analyze the model before optimizing. Figure 17 shows the power density as a function of the current density for several temperatures with the oxygen pressure fixed at 0.21 atm and hydrogen pressure fixed at 1 atm. The same pattern observed with the SOFC is also observed here: the maximum power tends to increase with the temperature. However, the output power and the working current density are obviously much lower than in the high temperature fuel cell. Figure 18 shows the influence of each loss. These are much more visible in the low temperature

fuel cell due to the evidence of a concentration over-potential limiting the current density by taking the power to zero.

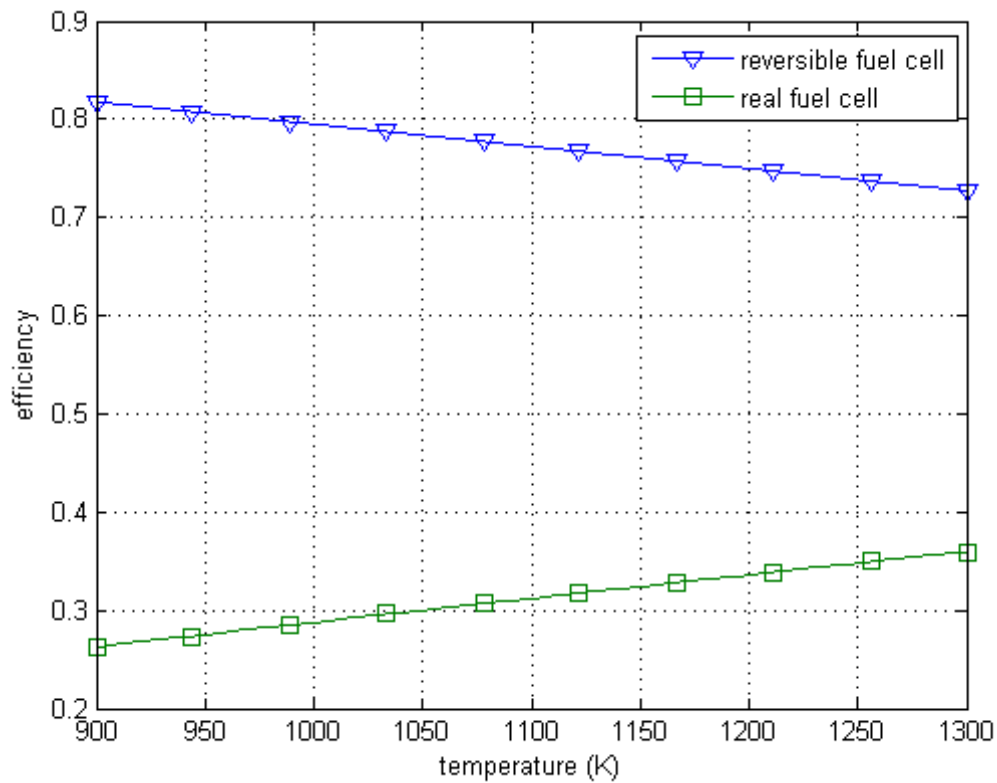


Figure 16. Efficiency of the reversible and real fuel cells

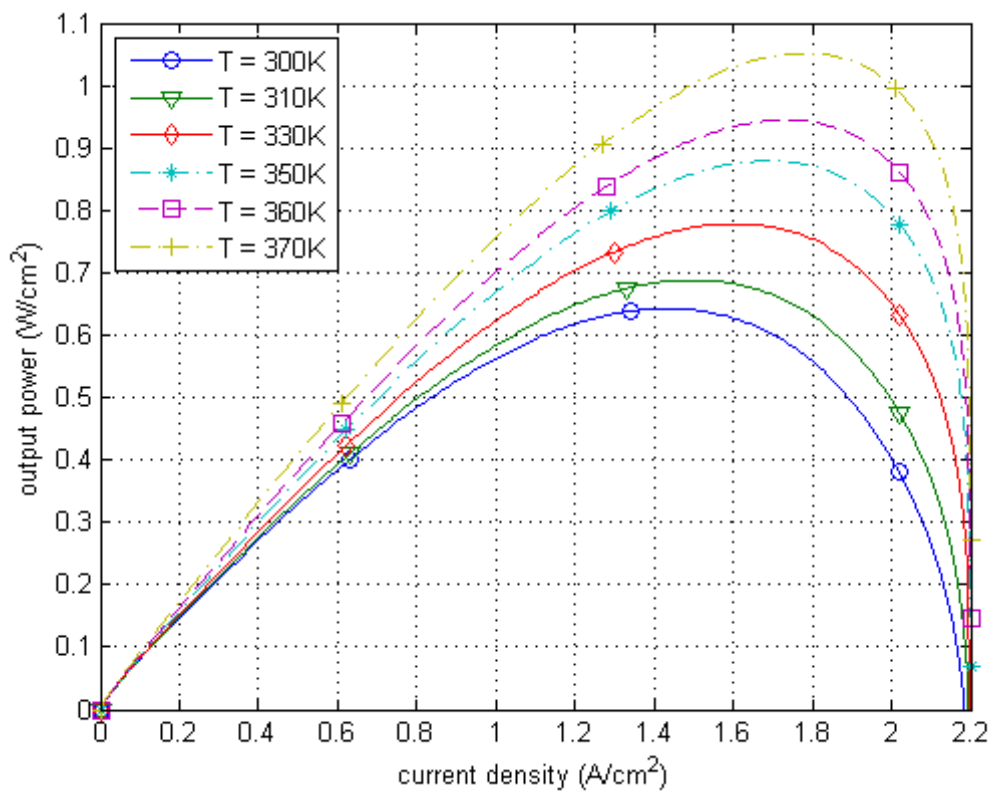


Figure 17. Power density as a function of current density for several temperatures

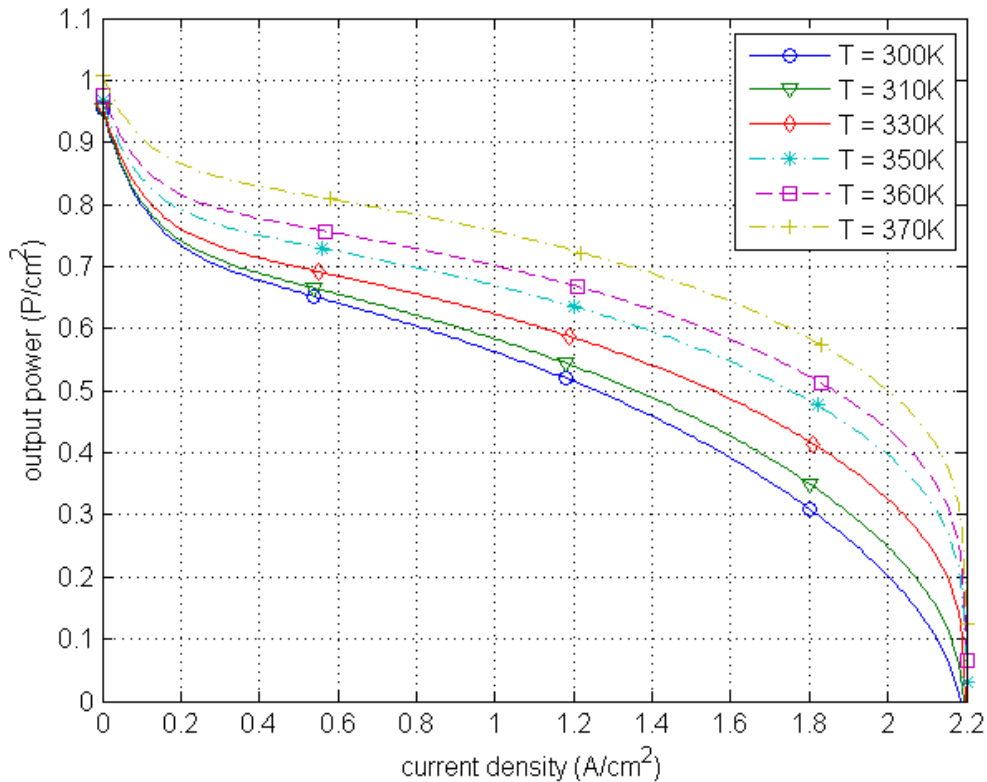


Figure 18. Output voltage as a function of current density for several temperatures

We proceed with the single-objective optimization. We perform optimization for the pressures of oxygen, hydrogen, temperatures and humidification coefficient  $\lambda$ . We then leave the oxygen pressure at 21% of the cathode pressure and optimize the parameters; this setup is analogous to saying we are using atmospheric air (only compressed, if necessary).

Tables 7 and 8 show the optimum values obtained by two single-objective optimizations and thus it is noticeable that the control over the oxygen pressure is more desirable than the control of the cathode pressure, as if one is able to control the oxygen, it has influence on the fuel cell reaction itself.

Table 7. PEMFC optimum values (pure oxygen at 1 atm cathode pressure)

Variable	Optimum
Temperature [K]	370
O <sub>2</sub> pressure [atm]	0.6853
H <sub>2</sub> pressure [atm]	3
Humidifying coefficient [ - ]	24
Current density [A/cm <sup>2</sup> ]	1.8125
Power [W/cm <sup>2</sup> ]	1.2016

Table 8. PEMFC optimum values (atmospheric air)

Variable	Optimum
Temperature [K]	370
O <sub>2</sub> pressure [atm]	0.63
H <sub>2</sub> pressure [atm]	3
Cathode pressure [atm]	3
Humidifying coefficient [ - ]	24
Current density [A/cm <sup>2</sup> ]	1.7842
Power [W/cm <sup>2</sup> ]	1.1138

We now solve the optimization algorithm for various temperatures and create a profile, like in the SOFC case. This graph is shown in Figure 19.

We calculate the efficiency of the real fuel cell and compare it to the reversible fuel cell. As shown in Figure 20, just like the SOFC case, even though the reversible efficiency decreases with temperature, the real efficiency increases and even though is higher than the efficiency of the SOFC, it is still very low.

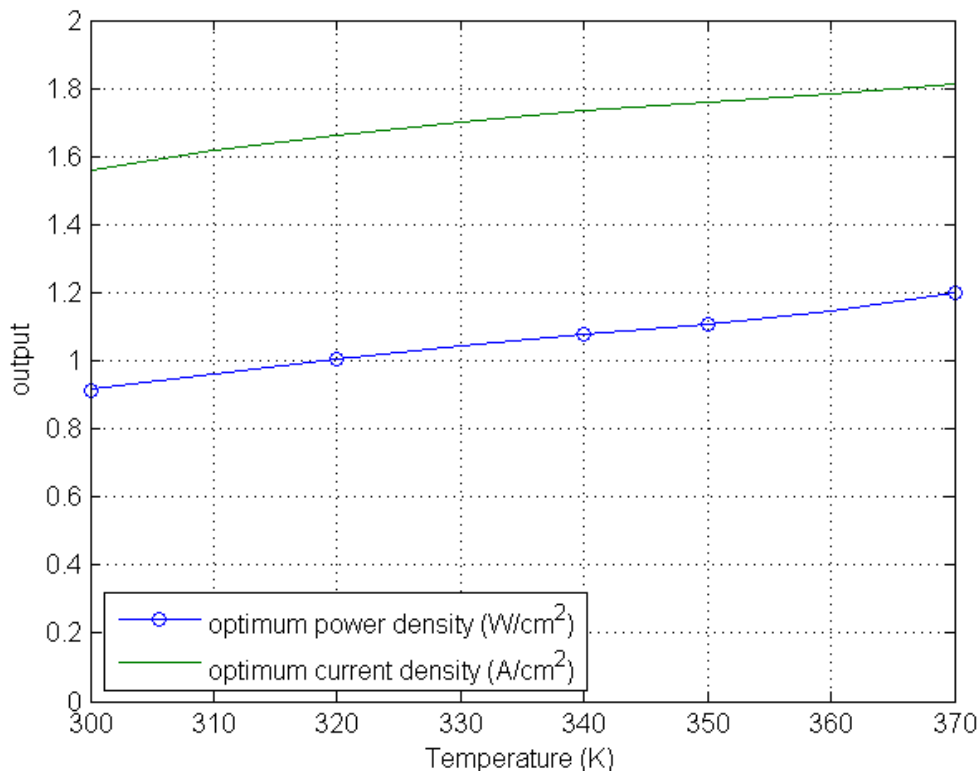


Figure 19. Optimum power and current density as a function of temperature

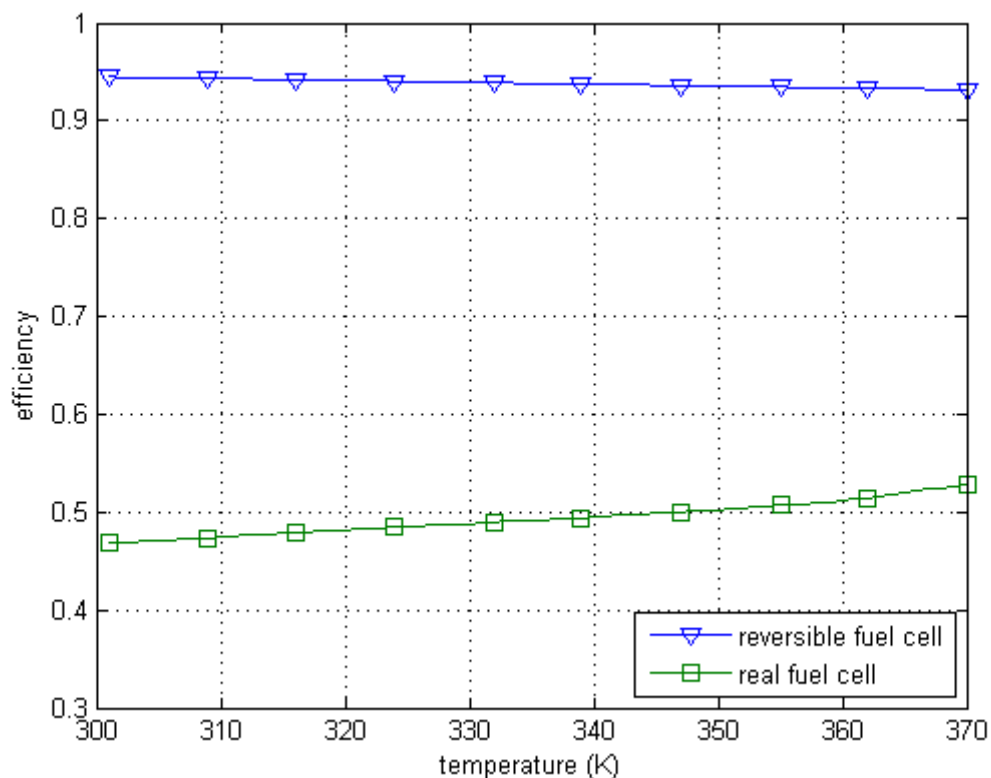


Figure 20. Reversible and real fuel cell efficiencies

## 6. Recommendations and conclusions

In this study, we made several contributions to the state of art in fuel cell modeling. First, we have shown a Pareto-front of plausible parameters for a better design of a fuel cell. We took into consideration the minimization of the pressure applied to the fuel cell, which should reduce stresses in the membrane that cause cracks. We have also shown that even if the efficiency of a high temperature fuel cell is lower than a low temperature fuel cell, its power output is still likely to be higher. We have shown that the multi-objective genetic algorithm is a powerful tool for design. Additionally, we have analyzed the optimum points of a fuel cell.

There is much work that needs to be done. The water management is a big problem in the fuel cell performance; further research in this area is needed. This paper has addressed the optimization and performance of a single fuel cell; the methodology should be extended to a stack of fuel cells.

## Acknowledgement

The lead author is grateful to the Ministry of Education of Brazil and the Brazilian Federal Agency for the Support and Evaluation of Higher Education (CAPES) for funding his studies at Washington University in St. Louis, USA.

## References

- [1] T. E. Springer, T. A. Zawodzinski, and S. Gottesfeld, "Polymer Electrolyte Fuel Cell Model," *J. Electrochem. Soc.*, vol. 138, no. 8, pp. 2334–2342, Aug. 1991.
- [2] A. V. Akkaya, "Electrochemical model for performance analysis of a tubular SOFC," *International Journal of Energy Research*, vol. 31, no. 1, pp. 79–98, 2007.
- [3] F. Zhao and A. V. Virkar, "Dependence of polarization in anode-supported solid oxide fuel cells on various cell parameters," *Journal of Power Sources*, vol. 141, no. 1, pp. 79–95, Feb. 2005.
- [4] P. A. Ramakrishna, S. Yang, and C. H. Sohn, "Innovative design to improve the power density of a solid oxide fuel cell," *Journal of Power Sources*, vol. 158, no. 1, pp. 378–384, Jul. 2006.
- [5] D. M. Bernardi and M. W. Verbrugge, "A Mathematical Model of the Solid Polymer Electrolyte Fuel Cell," *J. Electrochem. Soc.*, vol. 139, no. 9, pp. 2477–2491, Sep. 1992.
- [6] H. Ben Moussa, B. Zitouni, K. Oulmi, B. Mahmah, M. Belhamel, and P. Mandin, "Hydrogen consumption and power density in a co-flow planar SOFC," *International Journal of Hydrogen Energy*, vol. 34, no. 11, pp. 5022–5031, Jun. 2009.
- [7] P. Costamagna, A. Selimovic, M. Del Borghi, and G. Agnew, "Electrochemical model of the integrated planar solid oxide fuel cell (IP-SOFC)," *Chemical Engineering Journal*, vol. 102, no. 1, pp. 61–69, Aug. 2004.
- [8] Y. Lin and S. B. Beale, "Performance predictions in solid oxide fuel cells," *Applied Mathematical Modelling*, vol. 30, no. 11, pp. 1485–1496, Nov. 2006.
- [9] H. Huang, M. Nakamura, P. Su, R. Fasching, Y. Saito, and F. B. Prinz, "High-Performance Ultrathin Solid Oxide Fuel Cells for Low-Temperature Operation," *J. Electrochem. Soc.*, vol. 154, no. 1, pp. B20–B24, Jan. 2007.
- [10] H. Yahiro, Y. Baba, K. Eguchi, and H. Arai, "High Temperature Fuel Cell with Ceria- Yttria Solid Electrolyte," *J. Electrochem. Soc.*, vol. 135, no. 8, pp. 2077–2080, Aug. 1988.
- [11] J. T. Pukrushpan, H. Peng, and A. G. Stefanopoulou, "Control-Oriented Modeling and Analysis for Automotive Fuel Cell Systems," *Journal of Dynamic Systems, Measurement, and Control*, vol. 126, no. 1, p. 14, 2004.
- [12] J. C. Amphlett, R. M. Baumert, R. F. Mann, B. A. Peppley, P. R. Roberge, and T. J. Harris, "Performance Modeling of the Ballard Mark IV Solid Polymer Electrolyte Fuel Cell I . Mechanistic Model Development," *J. Electrochem. Soc.*, vol. 142, no. 1, pp. 1–8, Jan. 1995.
- [13] P. Costamagna and K. Honegger, "Modeling of Solid Oxide Heat Exchanger Integrated Stacks and Simulation at High Fuel Utilization," *J. Electrochem. Soc.*, vol. 145, no. 11, pp. 3995–4007, Nov. 1998.
- [14] J. H. Lee and T. R. Lalk, "Modeling fuel cell stack systems," *Journal of Power Sources*, vol. 73, no. 2, pp. 229–241, Jun. 1998.
- [15] M. J. Khan and M. T. Iqbal, "Modelling and Analysis of Electro-chemical, Thermal, and Reactant Flow Dynamics for a PEM Fuel Cell System," *Fuel Cells*, vol. 5, no. 4, pp. 463–475, 2005.

- [16] L. Matamoros and D. Brüggemann, "Simulation of the water and heat management in proton exchange membrane fuel cells," *Journal of Power Sources*, vol. 161, no. 1, pp. 203–213, Oct. 2006.
- [17] J. J. Durillo, A. J. Nebro, and E. Alba, "The jMetal framework for multi-objective optimization: Design and architecture," in *2010 IEEE Congress on Evolutionary Computation (CEC)*, 2010, pp. 1-8.
- [18] F. Kursawe, "A Variant of Evolution Strategies for Vector Optimization," in *Proceedings of the 1st Workshop on Parallel Problem Solving from Nature*, London, UK, UK, 1991, pp. 193–197.
- [19] S. Pasricha and S. R. Shaw, "A dynamic PEM fuel cell model," *IEEE Transactions on Energy Conversion*, vol. 21, no. 2, pp. 484 – 490, Jun. 2006.
- [20] J. Zhang, Z. Xie, J. Zhang, Y. Tang, C. Song, T. Navessin, Z. Shi, D. Song, H. Wang, D. P. Wilkinson, Z.-S. Liu, and S. Holdcroft, "High temperature PEM fuel cells," *Journal of Power Sources*, vol. 160, no. 2, pp. 872–891, Oct. 2006.
- [21] A. Vaudrey, P. Baucour, F. Lanzetta, and R. Glises, "Detailed analysis of an endoreversible fuel cell : Maximum power and optimal operating temperature determination," arXiv:0905.2871, May 2009.
- [22] T. Lu, "Numerical simulation of a flat-tube high power density solid oxide fuel cell," University of Pittsburgh, Pittsburgh, 2005.
- [23] W. Wagner and A. Pruss, *International Equations for the Saturation Properties of Ordinary Water Substance: Revised According to the International Temperature Scale of 1990*. American Chemical Society, 1993.
- [24] V. B. D. Živko, "Analysis of individual PEM fuel cell operating parameters for design of optimal measurement and control instrumentation," pp. 385–99.
- [25] R. P. O'Hayre, *Fuel cell fundamentals*. John Wiley & Sons, 2006.
- [26] D. E. Goldberg, *Genetic Algorithms in Search, Optimization and Machine Learning*, 1st ed. Boston, MA, USA: Addison-Wesley Longman Publishing Co., Inc., 1989.
- [27] N. Srinivas and K. Deb, "Multiobjective Optimization Using Nondominated Sorting in Genetic Algorithms," *Evolutionary Computation*, vol. 2, pp. 221–248, 1994.
- [28] D. W. C. Abdullah Konak, "Multi-objective optimization using genetic algorithms: A tutorial," *Reliability Engineering & System Safety*, no. 9, pp. 992–1007.
- [29] K. Deb, A. Pratap, S. Agarwal, and T. Meyarivan, "A fast and elitist multiobjective genetic algorithm: NSGA-II," *IEEE Transactions on Evolutionary Computation*, vol. 6, no. 2, pp. 182 – 197, Apr. 2002.



**Gustavo Marques Hobold** is a Mechanical Engineering B.S. student at Federal University of Santa Catarina, Brazil, and exchange student at Washington University in St. Louis, USA, where he is funded by the Brazilian government to study advanced engineering coursework. His research interests include numerical optimization, heat transfer, thermodynamics and fluid mechanics and their application to energy generation and aerospace engineering.  
E-mail address: hobold@lepten.ufsc.br



**Ramesh K. Agarwal** received PhD in aeronautical sciences from Stanford University in 1975. His research interests are in the theory and applications of Computational Fluid Dynamics (CFD) to study the fluid flow problems in aerospace and renewable energy systems. He is currently the William Palm Professor of Engineering in department of Mechanical Engineering and Materials Science at Washington University in St. Louis, MO, USA. He is a Fellow of ASME, AIAA, IEEE, and SAE.  
Email address: rka@wustl.edu

